

Current Status of Nuclear Data Processing Code NECP-Atlas

Tiejun Zu*, He Wu, Yihan Huang, Ning Xu, Wen Yin, Liangzhi Cao, Hongchun Wu
School of Nuclear Science and Technology, Xi'an Jiaotong University, Xi'an, Shaanxi 710049, China

*Corresponding author: tiejun@mail.xjtu.edu.cn

1. Introduction

The task of nuclear data processing code is to process the evaluated nuclear data into a specific format data library for neutronics codes.

NECP-Atlas is a nuclear data processing code independently developed by Xi'an Jiaotong University. The code currently has all the basic functions of traditional nuclear data processing codes, including: resonance reconstruction and linearization, doppler broadening, effective self-shielded cross-section calculation in unresolved resonance region, probability table calculation, thermal scattering cross-section calculation, neutron and photon multi-group constant calculation, etc.; can output continuous energy data library with ACE format for Monte Carlo codes and multi-group data library for deterministic calculation codes. The calculation models of each module can be found in reference [1].

This paper mainly introduces the recent development process in NECP-Atlas, including the processing of GNDS format evaluated nuclear data library, the calculation method of photon-atom coherent scattering differential cross section based on molecular interference function, and the displacement damage cross section caused by light nuclei.

2. Research Progress of Nuclear Data Processing Code NECP-Atlas

2.1 The Processing of GNDS Format Evaluated Nuclear Data Library

At present, the latest version of the evaluated nuclear data library in the world adopts the traditional ENDF-6 format and the latest GNDS format. Different from the traditional evaluated nuclear data library stored in the ENDF-6 format, the GNDS format uses the modern computer standard language, such as XML language, to store the evaluated nuclear data, which has better readability, scalability, and compatibility.

NECP-Atlas has developed a data storage format compatible with the GNDS format based on the original function of processing the ENDF-6 format evaluated nuclear data library. As shown in Fig.1, NECP-Atlas has developed the reading function of the evaluated nuclear data library in GNDS. NECP-Atlas can read and parse the evaluated nuclear data library in GNDS format stored in XML language, convert and store data in Root-Lib, the basic data structure used for data transmission among different modules of NECP-Atlas. Subsequently, the data can be used for subsequent

nuclear data processing procedure. Finally, NECP-Atlas can process the evaluated nuclear data library in GNDS format to produce ACE format data library and multi-group data library. More details for the capacity for processing GNDS format libraries can be referred to the paper [2].

2.2 The Calculation Method of Photon-atom Coherent Scattering Differential Cross Section Based on Molecular Interference Function

Photon has important applications in nuclear energy systems, such as nuclear reactor photon heating calculation and radiation shielding calculation etc., which need to consider the influence of photon. The basic physical principle of X-ray diffraction is the coherent scattering. The conventional calculation of the coherent scattering differential cross section adopts the independent atomic form factor approximation [3] to modify the Thomson scattering cross section, which can accurately calculate the coherent scattering differential cross section with high photon momentum transfer [4]. When the momentum transfer of the photon is low, the calculation of the coherent scattering differential cross section will have a large deviation, and the angular distribution of the coherent scattering secondary photon cannot be accurately described. Therefore, a more accurate method is needed to calculate the coherent scattering differential cross section of low energy photons. On the basis of the traditional independent atomic form factor approximation, the traditional coherent scattering differential cross section calculation method is extended to the low energy region by considering the molecular interference effect.

2.2.1 Independent Atomic Form Factor Approximation

The differential elastic scattering cross section of a photon and a free electron can be expressed by the Thomson scattering:

$$\frac{d\sigma_{Th}}{d\mu} = \frac{3\sigma_{Th}}{8} (1 + \mu^2) \quad (1)$$

where, $\frac{d\sigma_{Th}}{d\mu}$ represents Thomson differential scattering cross section; σ_{Th} represents Thomson cross section; μ represents the mean scattering angle cosine.

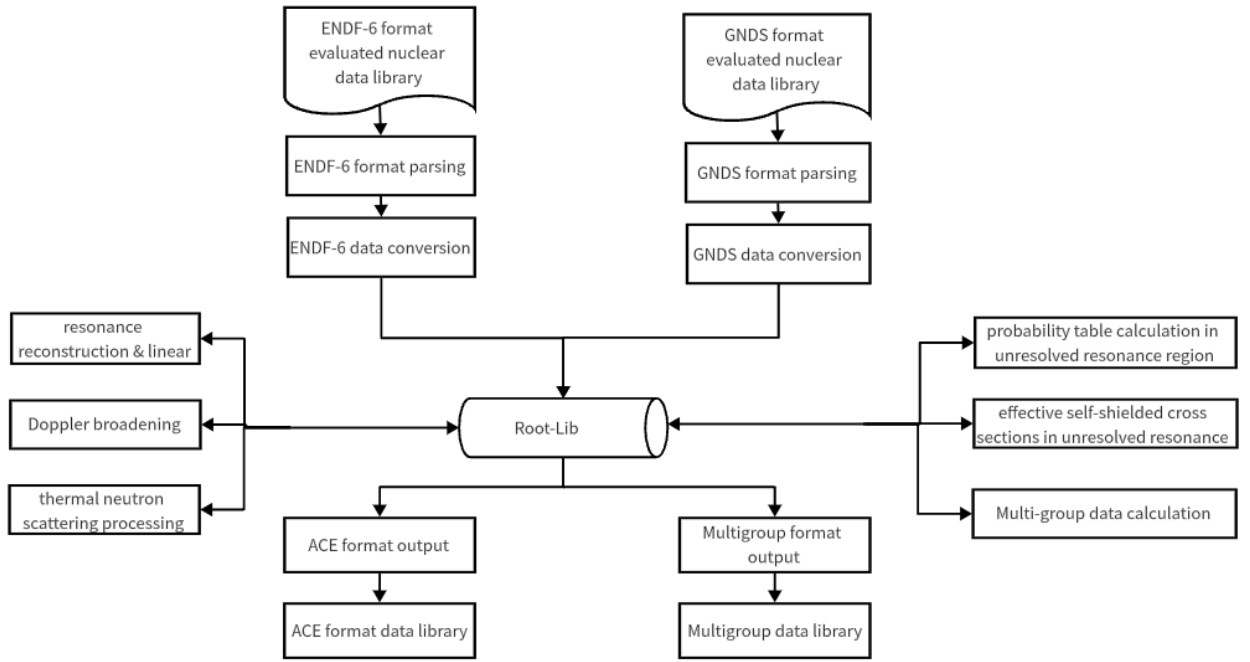


Fig. 1. The nuclear data processing flowchart of NECP-Atlas

Different from a free electron described by Thomson scattering equation, electrons outside the nucleus are bound by the nucleus, and the energy of electrons in different orbitals is different, that is, electrons outside the nucleus have electron density distribution. For all elements except hydrogen, the neutral atom has more than one electron outside its nucleus. Because of the above two reasons, the Thomson scattering equation cannot be used to calculate the coherent scattering differential cross section directly, so it needs to be modified to take into account the influence of the above two factors. At present, the most common correction method is the independent atomic form factor approximation method.

For an isolated atom, the distribution of electrons outside the nucleus is not affected by the distribution of electrons outside other nuclei, assuming that the distribution of electron density outside the nucleus is spherical symmetric, then the coherent scattering differential cross section can be expressed as:

$$\frac{d\sigma_{Coh}}{d\mu} = \frac{d\sigma_{Th}}{d\mu} |f(x, Z)|^2 \quad (2)$$

where, $\frac{d\sigma_{Coh}}{d\mu}$ represents the coherent scattering differential cross section; $f(x, Z)$ represents independent atomic form factor; x represents momentum transfer; Z represents the number of protons of the element.

The momentum transfer x can be expressed as:

$$x = \frac{\sin(\theta/2)}{\lambda} = \frac{m_e c^2}{2hc} \frac{2E}{m_e c^2} \sin \frac{\theta}{2} = 20.60744 * 2k \sqrt{\frac{1-\mu}{2}} \quad (3)$$

where, θ represents the scattering angle; m_e represents the rest mass of the electron; h represents Planck constant; c represents the speed of light; k represents the energy of incident photon in unit of rest energy of electron.

Using the independent atomic form factor to modify the Thomson scattering cross section can only consider the effect of electron density distribution inside isolated atoms on the coherent scattering differential cross section, but ignores the effect of intramolecular interference and intermolecular interference on the coherent scattering differential cross section. When calculating the coherent scattering differential cross section of molecules based on the independent atomic form factor approximation method, it is only necessary to weight the differential scattering cross section of each atom in the molecule according to nucleon density [5].

$$\frac{d\sigma_{coh,mol}^{IAM}(E)}{d\mu} = \frac{d\sigma_{Th}}{d\mu} \sum_i f_i^2(x, Z_i) \quad (4)$$

This approximate method is only suitable for calculating the coherent scattering differential cross section when the recoil momentum of photon is high. When the recoil momentum of photon is small, ignoring the intramolecular and intermolecular interference effects will affect the calculation accuracy of the angular distribution of coherent scattered secondary photons [6].

2.2.2 Molecular Interference Function Calculation

Molecular interference effect can be divided into intramolecular interference effect and intermolecular interference effect. Debye equation can be used to

calculate the atomic form factor considering intramolecular interference effect:

$$F_{\text{Debye}}(x) = \sum_{ij} f_i(x, Z_i) f_j(x, Z_j) \frac{\sin 4\pi x r_{ij}}{4\pi x r_{ij}} \quad (5)$$

where, $f_i(x, Z_i)$ and $f_j(x, Z_j)$ represent the independent atomic form factors of elements i and j respectively; x represents photon momentum transfer; r_{ij} represents the distance between atom i and atom j within the molecule.

The intermolecular interference effect is generally corrected by molecular interference function [7], which can be expressed as:

$$S(x) = \frac{\sum_{ij} f_i(x) f_j(x) s_{ij}(x)}{\left(\sum_i f_i(x, Z_i)\right)^2} \quad (6)$$

where, $s_{ij}(x)$ represents the partial molecular interference function.

When the molecular structure is known, the partial molecular interference function can be calculated [8] by molecular dynamics simulation:

$$s_{ij}(x) = 4\pi\rho_0 \int_0^\infty r^2 (g_{ij}(r) - 1) \frac{\sin 4\pi x r}{4\pi x r} dr \quad (7)$$

where, ρ_0 represents the atomic number density, that is, the number of atoms per unit volume; $g_{ij}(r)$ represents the radial distribution function, that is, the ratio of the local density of an atom of atomic type j in a shell of dr thickness at a distance r around a reference atom i to the density of the reference atom.

The atomic form factor considering intramolecular interference effects and intermolecular interference effects can be expressed as:

$$F(x) = \left[\sum_{ij} f_i(x, Z_i) f_j(x, Z_j) \frac{\sin 4\pi x r_{ij}}{4\pi x r_{ij}} \right] * S(x) \quad (8)$$

By using the atomic form factor calculated by Eq. (8) to modify the Thomson scattering cross section, the photon-atomic coherent scattering differential cross section considering the molecular interference effect can be obtained:

$$\frac{d\sigma_{\text{coh, mol}}^M}{d\mu} = \frac{d\sigma_{\text{Th}}}{d\mu} F(x) \quad (9)$$

2.3 Displacement Damage Cross-section Caused by Light Nuclei

When nuclear materials are exposed to high-energy light nuclear radiation, their mechanical properties will change significantly. It is necessary to accurately evaluate the radiation level of these materials, and DPA is usually used to evaluate the radiation level of

materials. In order to calculate the DPA of the irradiated material after a period of time, it is first necessary to calculate the displacement damage cross section of the irradiated material.

In the previous version of the NECP-Atlas code, the calculation function of the displacement damage cross section of neutrons, electrons and photons in elemental materials and the displacement damage cross section of neutrons in compound materials has been realized [9]. It can be seen from previous studies that displacement damage cross section can be calculated by the following expression:

$$\sigma_D(E) = \int_0^{T_m} v(T) \frac{d\sigma}{dT} dT \quad (10)$$

Where, T_m represents the maximum energy of the recoil nuclear generated; $d\sigma/dT$ represents differential scattering cross section; $v(T)$ represents the displacement damage function. Eq. (10) is also applicable to the calculation of displacement damage cross section of light nuclei. When calculating the differential scattering cross section of light nuclei, elastic scattering reaction and inelastic scattering are considered respectively. For the elastic scattering part, LNS equation, optical model and relativistic equation are used in the low energy, medium energy and high energy regions respectively. For the inelastic scattering part, the Monte Carlo code PHITS is used. In addition to the traditional NRT model, ARC model is also used to calculate the displacement damage function, and a new ARC model parameters are obtained based on the experimental data to improve the calculation accuracy. The parameters of the new model are shown in reference [10].

3. Verification of the new capacities

3.1 Verification of GNDS format processing

Using the latest ENDF/B-VIII.0 evaluated nuclear data library, NECP-Atlas was used to make two sets of ACE format libraries based on ENDF-6 format and GNDS format evaluated nuclear data library respectively, as shown in Fig.2. NECP-MCX, a Monte Carlo code independently developed by Xi'an Jiaotong University, was used to calculate a total of 300 ICSBEP benchmark problems of different fuels, different devices and different geometries [11], and the calculated deviation of the two sets of data libraries was compared as shown in Fig.3.

As can be seen from the figure, the maximum deviation of calculation results between GNDS format and ENDF-6 format is 46pcm. And comparing the calculation results of two different evaluated data library formats, it can be found that the deviation of most calculation results is less than 5pcm.

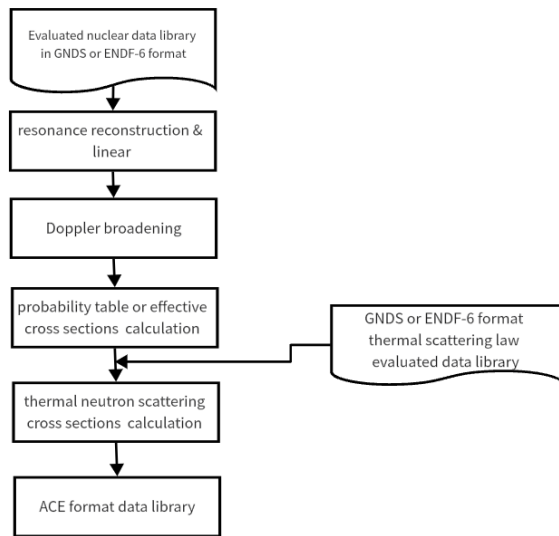


Fig. 2. The flowchart of generating ACE libraries.

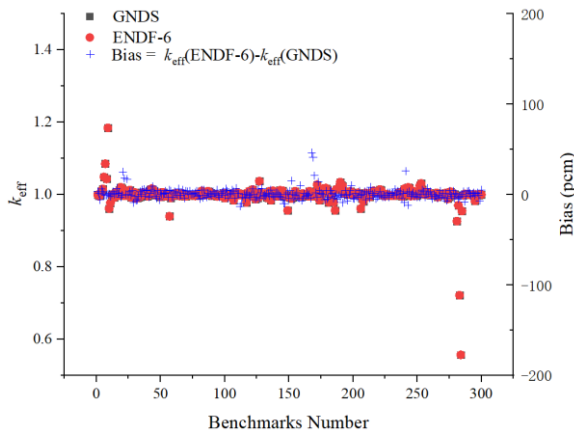


Fig. 3. Results of ICSBEP benchmarks.

This proves that NECP-Atlas can process GNDs evaluated nuclear data library correctly and generate ACE data library correctly.

3.2 Verification of Photon-atom Coherent Scattering Differential Cross Section Based on Molecular Interference Function

3.2.1 Molecular Interference function Calculation

Molecular interference function can be calculated by molecular dynamics simulation code. In this paper, the TIP4P/2005 model [12] was used for molecular dynamics simulation of water molecule. OPLS-AA force field was used in the simulation of water molecules, and GROMACS molecular dynamics code [13] was used to simulate water molecules, and the radial distribution function between atoms of water molecules was obtained as shown in Fig.4.

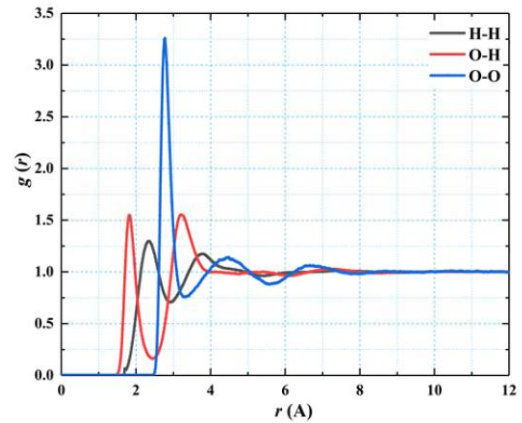


Fig. 4. The radial distribution function of water.

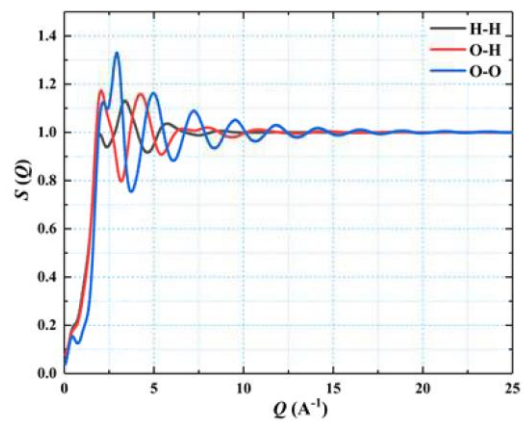


Fig. 5. Partial molecular interference function of water.

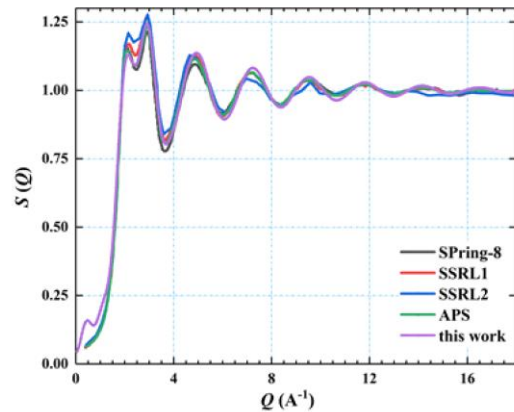


Fig. 6. The molecular interference function of water.

Based on the radial distribution function of water molecules calculated in Fig.4, the Partial molecular interference function of water molecules can be calculated using Eq. (7), as shown in Fig5. Finally, by weighting the partial molecular interference function, the molecular interference function of water molecules can be obtained, as shown in Fig.6. Among them, the molecular interference function simulation results of water molecules were compared with the experimental measurement results [14,18], and it can be seen that the molecular interference function obtained based on

molecular dynamics simulation is in good agreement with the experimental measurement results, which can be used to modify the independent atomic form factor and obtain the atomic form factor considering the molecular interference effect.

3.2.2 Analysis of the Influence of Molecular Interference Effect on the Angular Distribution of Coherent Scattering

In order to verify the influence of molecular interference effect on the angular distribution of coherent scattering, a set of photon-atom ACE format data library using independent atomic form factor approximation and considering molecular interference effect was produced respectively.

The device in Fig.7 was simulated by Monte Carlo code, and the imaging effect of water was compared and analyzed. The photon source in the device is an X-ray tube with a tube voltage of 100kV. The energy spectrum of the photon source is shown in Fig.8. The photon source is 100 cm away from the center of the sample (SAD). The distance of the photon source from the detection plate is 153.6 cm (SDD). And the size of the cube is $0.5 \times 0.5 \times 0.5 \text{ cm}^3$. The width of the detection plate is 41 cm [6].

Fig.9 respectively compares the simulated results of water molecule scattering imaging using independent atomic form factor approximation and considering molecular interference effect with the calculated results of G. Poludniowski [6]. The horizontal position 0 in Fig.9 corresponds to the center of the plate in Fig.7. It can be seen that the results of water molecular imaging in this paper are in good agreement with those calculated by G. Poludniowski. Through the comparative analysis of Fig.9(a) and Fig.9(b), it can be seen that there are obvious differences between the simulated results of water molecule scattering imaging when the molecular interference effect is considered or not. It can be seen from the imaging results that the forward scattering of coherent scattering is significantly reduced by considering the effect of molecular interference.

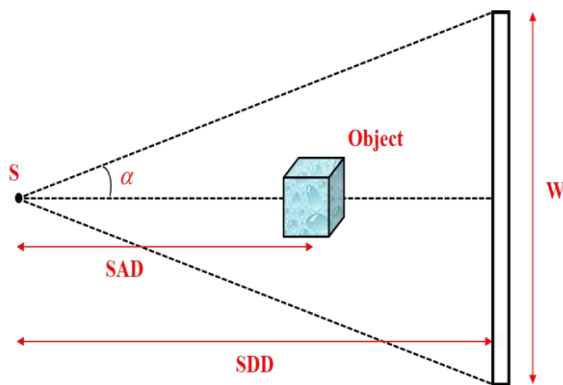


Fig. 7. Illustration of the imaging geometry.

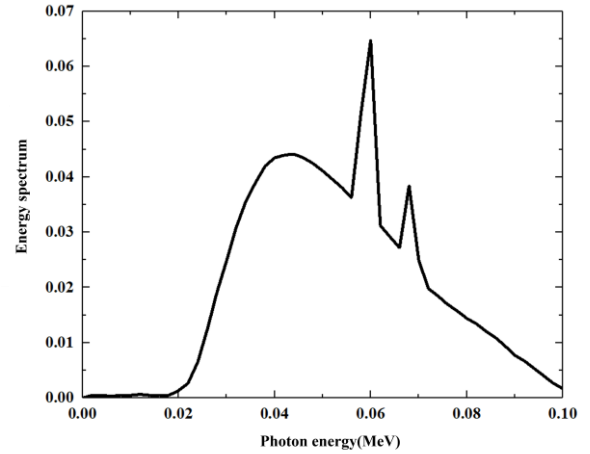
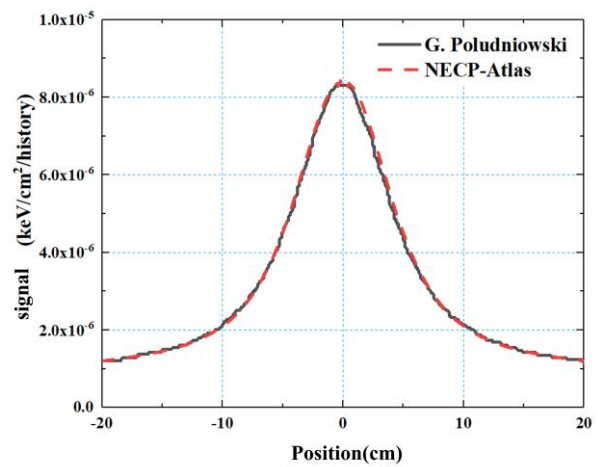
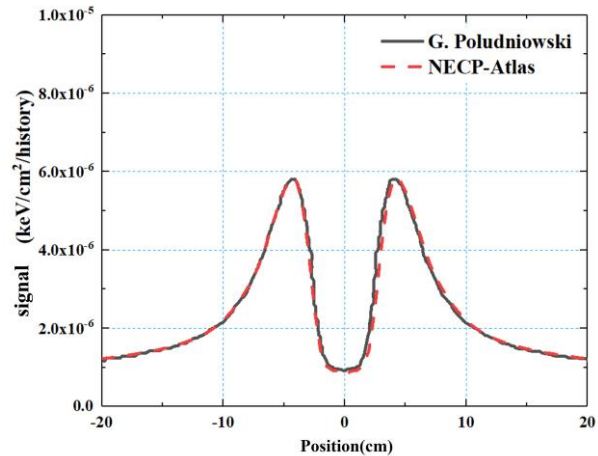


Fig. 8. Spectra of the photon source



(a) using the independent atom approximation



(b) using molecular interference model

Fig. 9. Comparison of the scattering images of water.

3.3 Verification of Displacement Damage Cross Section Caused by Light Nuclei

A large number of experimental results were selected as reference results to verify the calculation accuracy of light nuclear displacement damage cross section by NECP-Atlas. Fig.10 and Fig. 11 show the displacement damage cross section of protons and deuterons incident

on Fe and Cu, respectively. All the results represented by points in Fig.10 and Fig.11 are experimental results, while other results are calculated by NECP-Atlas. Among them, the calculation adopts NRT model, ARC model with model parameters given by Nordlund [19], and ARC model with newly fitted model parameters. It can be seen from the figures that ARC model with new fitting model parameters can greatly improve the calculation accuracy of the displacement damage cross section of light nuclei. The NRT model overestimates the displacement damage of the material in the full energy range. The ARC model using the model parameters given by Nordlund will underestimate the displacement damage of the material by proton irradiation at the high energy portion and deuteron irradiation at the full energy segment.

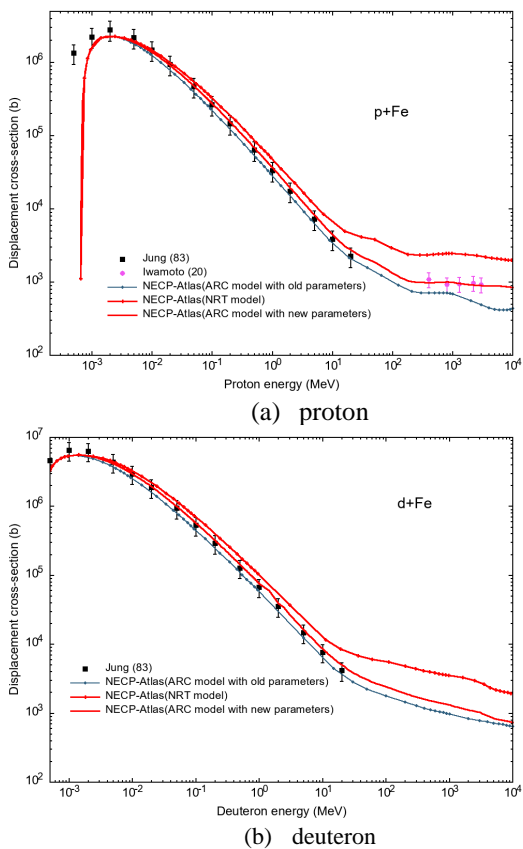


Fig. 10. The displacement cross section of Fe

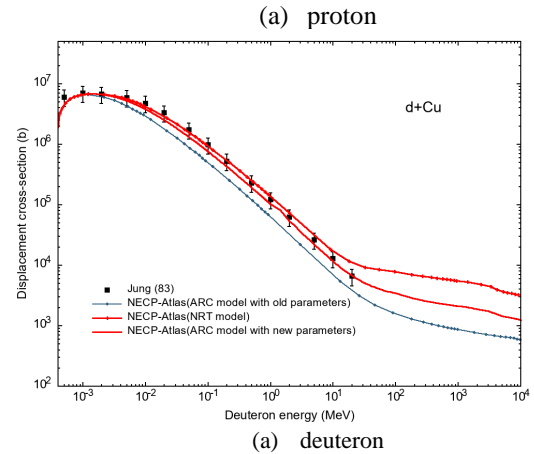
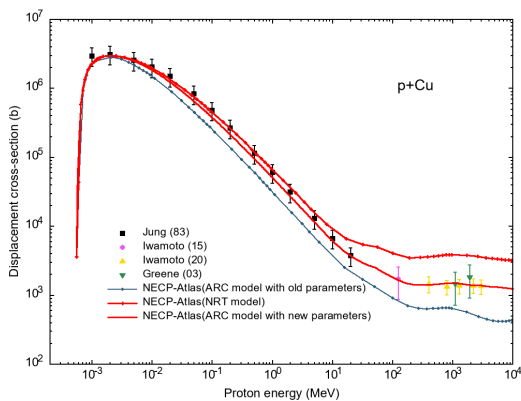


Fig. 11. The displacement cross section of Cu

4. Conclusions

This paper introduces the newly developed capacities in nuclear data processing code NECP-Atlas, including processing the GNDS format evaluated nuclear data libraries, calculating photon-atom coherent scattering cross section based on molecular interference function and displacement damage cross section of light nuclei. The capacities are verified. The numerical results show that the GNDS format evaluated nuclear data libraries can be correctly processed by NECP-Atlas, and used by neutronics simulation codes. NECP-Atlas can produce high-precision displacement damage cross section data and photon-atom data.

REFERENCES

- [1] Tiejun Zu, et al. NECP-Atlas: A new nuclear data processing code[J]. Annals of Nuclear Energy, 123:153-161, 2019.
- [2] Huang Y H, Zu T J, Cao L Z, et al. Capability of processing the GNDS format evaluated nuclear data in NECP-Atlas for neutronics calculations[J]. Progress in Nuclear Energy, 2022, 150: 8.
- [3] Cullen, Dermott E, John H. Hubbell and Lynn Kissel. EPDL 97: the Evaluated Photon Data Library[R], 1997.
- [4] Soper A K. Joint structure refinement of x-ray and neutron diffraction data on disordered materials: application to liquid water[J]. Journal of Physics: Condensed Matter, 19(335206), 2007.
- [5] Boke A. The effect of molecular interference on coherent scattering[J]. Journal of Balikesir University Institute of Science and Technology, 19(2), 2017.
- [6] G Poludniowski, P M Evans and S Webb. Rayleigh scatter in kilovoltage x-ray imaging: is the independent atom approximation good enough[J]. Physics in Medicine & Biology, 54(6931), 2009.
- [7] Jiahu Wang, Awadh N and Vedene H. Chemical binding and electron correlation effects in x - ray and high energy electron scattering[J]. The Journal of Chemical Physics, 101(4842). 1994.
- [8] Jon M. Sorenson, Greg Hura, Robert M. Glaeser, et al. What can X-ray scattering tell us about the radial distribution functions of water[J]. The Journal of Chemical Physics, 113(20):9149-9161. 2000.

- [9] Yin, W., et al. "Development and verification of heat production and radiation damage energy production cross section module in the nuclear data processing code NECP-Atlas." *Annals of Nuclear Energy* 144(2020):107544.
- [10] Wen Yin, A. Yu. Konobeyev, D. Leichtle, et al. Calculation of displacement damage cross-section for charged particles at energies up to 100 GeV [J]. *Journal of Nuclear Materials*, 573:154143, 2023.
- [11] Briggs J B. International handbook of evaluated criticality safety benchmark experiments[J]. Nuclear Energy Agency, NEA/NSC/DOC (95), 2004, 3: 1.
- [12] Abascal JL, Vega C. A general purpose model for the condensed phases of water: TIP4P/2005[J]. *The Journal of Chemical Physics*, 123(23):234505, 2005.
- [13] Van Der Spoel D, Lindahl E, Hess B, et al. GROMACS: fast, flexible, and free[J]. *Journal of Computational Chemistry*, 26(16): 1701-1718, 2005.
- [14] L. B. Skinner, C. J. Benmore, and J. B. Parise. Molecular arrangement in water: random but not quite[J]. *Journal of Physics: Condensed Matter*, 24(338001), 2012.
- [15] L. B. Skinner, C. J. Benmore, B. Shyam, et al. Structure of the floating water bridge and water in an electric field[J]. *Proceedings of the National Academy of Sciences*, 109(16463), 2012.
- [16] R. T. Hart, C. J. Benmore, J. C. Neuefeind, et al. Temperature dependence of isotopic quantum effects in water[J]. *Physical Review Letters*, 94(047801), 2005.
- [17] C. Huang, K. T. Wikfeldt, D. Nordlund, et al. Wide-angle X-ray diffraction and molecular dynamics study of medium-range order in ambient and hot water[J]. *Physical Chemistry Chemistry Physical*, 13: 19997-20007, 2011.
- [18] L. Fu, A. Bienenstock, and S. Brennan. X-ray study of the structure of liquid water[J]. *The Journal of Chemical Physics*, 131(234702), 2009.
- [19] Nordlund, K., et al. (2018). Improving atomic displacement and replacement calculations with physically realistic damage models. *Nat Commun.* 9: 1084.